Photonic Integrated Circuits for Electro-optic Microwave Frequency Multiplication and Frequency Translation: Spurious Harmonics Suppression by Design

Ramón Maldonado-Basilio and Trevor J. Hall
Photonic Technology Laboratory, University of Ottawa
800 King Edward Avenue, K1N 6N5, ON, Canada

Abstract— Various photonic circuit architectures for RF frequency multiplication and frequency translation are presented. Firstly a systematic design method for the suppression of unwanted harmonics produced by parallel phase modulator arrays is developed. The analyzed configuration comprises of N-parallel phase modulators electrically driven with a progressive $2\pi/N$ phase shift. For $N = 4$, the analyzed circuit is conceptually equivalent to the DP-MZM architecture available in $LiNbO_3$ technology. Improved implementations of some functions can be achieved for a larger number of phase modulators. Secondly, a photonic circuit architecture capable of implementing frequency up-conversion and frequency octo-tupling is proposed and verified by computer simulations. The circuit requires no DC-bias as the static phase shifts are introduced by using the intrinsic relative phase relations between the output and input ports of MMI couplers. The single side-band operation can be performed for a wide range of modulation index whilst the frequency octo-tupling requires a more specific modulation index. Last but never the least, a photonic circuit architecture featuring two-stage MZM architecture is proposed for frequency octo-tupling and 24-tupling. The analysis and simulations prove this cascade architecture is advantageous compared to the single-stage parallel MZM configuration with equivalent function because it requires 3-dB less power in RF drive.

1. INTRODUCTION

In the past two decades or so there has been a plethora of publications in the field of microwave photonics that have described essentially the same generalized Mach-Zehnderinterferometer (GMZI) circuit architecture: a $1 \times N$ splitter directly interconnected to a $N \times 1$ combiner via an array of N electro-optic $LiNbO_3$-based phase modulators; each GMZI adapted to particular design goals. The applications have generally been to single-side-band (SSB) modulation or electro-optic microwave signal frequency multiplication [1–3]. The difference between the circuits proposed have largely concerned variations of the static optical and electrical phase shifts required or the implementation of an equivalent circuit using standard Mach-Zehnder modulators (MZM) rather than individual phase-modulators as the basic building brick. After our latest investigations [4–6], in this work a methodology is presented that specifies the architecture required to meet specified design objectives such as the suppression of unwanted products. Moreover, it is shown how to use the intrinsic phase relations between the ports of splitters and combiners and specifically multi-mode interference couplers to implement the static optical phase shifts required by these circuits, thereby avoiding the need to apply static DC bias to the electro-optic modulators and the associated drift issues that otherwise require complex stabilization circuitry. Circuits capable of single-side-band suppressed-carrier modulation and frequency octo-tupling show a simulation performance equal to or better than results reported in the literature. In particular, a new cascade architecture implementation is reported that offers 50% lower optical insertion loss and 50% reduced RF power drive requirement compared to previously known circuits. While $LiNbO_3$ technology offers a mature solution to the small scale integration of MZM structures, this work anticipates photonic integrated circuits based on Si and/or InP material integration platforms emerging as the preferred choice. In this context the continuous advances made in improved speed, linearity, footprint, and energy consumption of electro-optic phase modulator devices in both material platforms augurs well for the future.

2. SPURIOUS HARMONIC SUPPRESSION BY DESIGN

Consider the array of N phase modulators in parallel shown in Figure 1(a), where each modulator is driven electrically by a cosinusoidal waveform with a progressive phase shift in units of $2\pi/N$. Using the Jacobi-Anger expansion, the complex amplitude of the field at the output of each PM can be expressed as:

$$\exp\left[im\cos\left(\theta+p\frac{2\pi}{N}\right)\right]=\sum\nolimits_{q=-\infty}^{\infty}\left[\exp\left(ipq\frac{2\pi}{N}\right)i^{q}J_{q}\left(m\right)\exp\left(iq\theta\right)\right] \tag{1}$$

where m is the modulation index; $\theta=\omega t$ and $p2\pi/N$ are the dynamic and static phase of the cosinusoidal electrical drive signal; the positive integer p denotes the index of the phase modulator in the array; $J_q(\cdot)$ is the Bessel function of the first kind with order q, and $i=\sqrt{-1}$ is the imaginary unit. The output of the combiner is:

$$\frac{1}{N}\sum\nolimits_{p=0}^{N-1}\left[a_p\exp\left(im\cos\left(\theta+p\frac{2\pi}{N}\right)\right)\right]=\sum\nolimits_{q=-\infty}^{\infty}\left[\tilde{a}_q i^{q}J_{q}\left(m\right)\exp\left(iq\theta\right)\right] \tag{2}$$

where the discrete Fourier transform:

$$\tilde{a}_q=\frac{1}{N}\sum\nolimits_{p=0}^{N-1}\left[a_p\exp\left(ipq\frac{2\pi}{N}\right)\right] \tag{3}$$

has entered the formulation. The sequence a_p denotes the complex weight of each phase modulator, which is preferably uni-modular to minimize loss of energy, i.e., a phase shift. It is observed that the sequence $\tilde{a}_q$ is periodic with period N. The importance of Equations (2) and (3) can be understood by considering first the simplest case for the weights, which is $a_p=1$ for $p=0,\,1,\,\ldots,\,N-1$. The discrete Fourier transform term (3) may be evaluated to yield:

$$\tilde{a}_q=\frac{1}{N}\frac{1-\exp\left(iq2\pi\right)}{1-\exp\left(iq\frac{2\pi}{N}\right)}=\frac{1}{N}\exp\left[iq\left(\frac{N-1}{N}\right)\pi\right]\frac{\sin\left(q\pi\right)}{\sin\left(q\frac{\pi}{N}\right)} \tag{4}$$

where the geometric series summation $\sum_{p=0}^{N-1}z^p=(1-z^N)/(1-z)$, with $z=\exp(iq2\pi/N)$, has been used. Applying L'Hôpital's rule to Equation (4), it is found that $\tilde{a}_0=1$for $q=0$, and $\tilde{a}_q=0$ for $q=1,\,2,\,\ldots,\,N-1$. The frequency domain sequence therefore suppresses periodically all harmonics except those that are multiples of N. One may take advantage of the shift theorem by modifying a given set of weights by the application of a progressive phase factor with increment $-q_0 2\pi/N$. That is $a_p\rightarrow a_p\exp(-ipq_0 2\pi/N)$ and hence:

$$\tilde{a}_q\rightarrow\frac{1}{N}\sum\nolimits_{p=0}^{N-1}\left[a_p\exp\left(ip\left(q-q_0\right)\frac{2\pi}{N}\right)\right]=\tilde{a}_{q-q_0} \tag{5}$$

The origin of the frequency domain sequence can be shifted therefore to position q_0 by a progressive phase shift of the light exciting the phase modulators with increment $-q_0 2\pi/N$. For the special case $a_p=1$ and integer q_0, $\tilde{a}_{q-q_0}$ is zero for each order except $q=q_0+rN$, where r is an integer. The design approach hence simplifies to the determination of a configuration of coefficients that suppresses specific harmonic orders while it maximises the harmonic orders of interest. An equivalent interpretation for the suppression function is found by expressing (3) as $\tilde{a}_q=(1/N)\sum_{p=0}^{N-1}[a_p z^p]$, where $z=\exp(iq2\pi/N)$ and then $\tilde{a}_q=f(\exp(iq2\pi/N))$ where:

$$f\left(z\right)=\frac{1}{N}\sum\nolimits_{p=0}^{N-1}a_p z^p=\frac{1}{N}a_0\prod_{j=1}^{N}\left(1-\frac{z}{z_j}\right) \tag{6}$$

The value of the suppression function f on the unit circle determines the weighting of the harmonics generated by the phase modulators. Note that the zeroes z_j of the suppression function may be placed anywhere in the complex plane. However, it is preferable that $|a_p|=1$ in which case the distribution of zeros is constrained. A design approach based on the application of a suppression function to minimize unwanted harmonics wherever is needed constitutes one of the main assets of the GMZI architecture. Since the process does not depend upon the modulation index, the linearity of the N-parallel phase modulators array is maintained and each PM can be driven at moderate input powers. Furthermore, for an even number of phase modulators, there will be pairs of phase modulators in differential drive, leading to an equivalent parallel MZM interpretation.

The operation of the N-parallel phase modulator array designed according to the approach presented here is verified by computer simulations using the Virtual Photonics Inc. (VPI) software

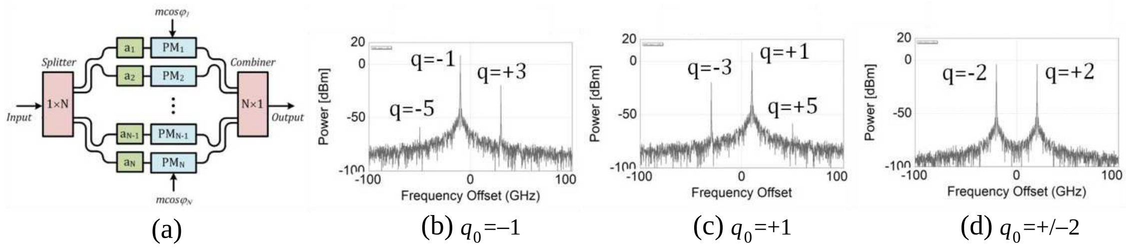

Figure 1: (a) Schematic diagram of a GMZI. (b)–(d) Simulated output for various design conditions in an array offour phase modulators: lower SSB, upper SSB, and frequency quadrupling after an square law photo-detector.

package. For simplicity, arrays comprising four phase modulators are shown as illustrative examples, although the design method holds for any number of modulators. A continuous wave DFB laser diode at 1550 nm, line-width of 200 kHz and power of 10 mW is used as the optical input. Optical phase shifters are used to model the uni-modular complex coefficients a_p, whereas cascaded Y-branches are used as the input $1 \times N$ splitter and output $N \times 1$ coupler. The cosinusoidal drive signals at the input of each of the four phase modulators have a frequency of 10 GHz and progressive electrical phase shifts φ_p equal to 0, $+\pi/2$, $+\pi$, and $+3\pi/2$, respectively. To achieve single-side-band modulation, for instance, the coefficient $q_0 = -1$ and the lowest order unsuppressed harmonics are -9, -5, -1, $+3$, and $+7$. In this case, the required optical weights a_p also have a progressive phase shifts of 0, $+\pi/2$, $+\pi$, and $+3\pi/2$, respectively. The quadrature driving signals to each upper and lower pair of MZM generate a composite spectrum comprising an optical carrier with a main harmonic located 10 GHz off the carrier frequency plus secondary modulation harmonics. In line with the design approach developed above, constructive interference by the imposed optical phase shifts benefits the lower order harmonic located 10 GHz to the left of the optical carrier. Due to destructive interference, other harmonics including the optical carrier are suppressed. In the equivalent $LiNbO_3$-based DP-MZM configuration, the same SSB modulator can be achieved by biasing the inner MZMs and outer MZI at the minimum- and half-transmission points, respectively. Following the presented design approach, other functions such as upper single-side-band modulation ($q_0 = +1$), frequency quadrupling ($q_0 = \pm 2$), and frequency octupling ($q_0 = 0$ with the drive level adjusted to suppress the carrier) can be achieved. Optical spectra obtained at the output of the generalized Mach-Zehnder interferometer (GMZI) comprising of four modulators array associated to the above mentioned functions are shown in Figure 1(b) to Figure 1(d). Note that the frequency multiplication is obtained after the output of the proposed architecture is passed through a square-law photo-detector.

3. SSB AND FREQUENCY OCTO-TUPLING

Figure 2(a) provides a schematic diagram of a circuit capable of the dual function of either millimeter wave generation by frequency octo-tupling a microwave RF input signal or frequency up-conversion to the optical domain of an RF input signal in the electronic domain by carrier suppressed SSB modulation. The latter being equivalent to the modulation of an optical carrier by baseband in-phase and quadrature (I&Q) signals. As illustrated in the schematic diagram, the 1×2 symmetric splitter together with the 2×1 symmetric combiner forms an outer MZI with two arms. Each arm itself contains an inner MZI sub-circuit formed by a 2×2 MMI splitter (with one input port unused) interconnected with a 2×2 MMI combiner, and linear electro-optic phase modulators in each arm that are differentially driven. The outer MZI is arranged to have two separate output ports, namely E_1 & E_2, and D. In one output, the two opposing ports (d_2) to the two input ports (a_1) are combined in a symmetric 2×1 MMI and provide the frequency octo-tupling of the RF input signal after a square-law photo-detector. On the other hand, the two remaining ports (d_1) are combined in a 2×2 MMI and provide the upper (E_1) and lower (E_2) SSB modulation. Following a transfer matrix approach to represent each building block in the proposed design, the operation of the single-side-band modulator can be described by:

$$E_1 = \frac{1}{2}\left[i \sin\left(\pi v_I / v_\pi\right) + \sin\left(\pi v_Q / v_\pi\right)\right] A \approx \frac{1}{2} i\pi\left(v^* / v_\pi\right) A \tag{7}$$

$$E_2 = \frac{1}{2}\left[-i\sin\left(\pi v_I/v_\pi\right) + \sin\left(\pi v_Q/v_\pi\right)\right]A \approx -\frac{1}{2}i\pi\left(v/v_\pi\right)A \tag{8}$$

where v_I and v_Q are the in-phase and quadrature components of the complex signal $v = v_I + iv_Q$ supplied to upper and lower MZIs, v_π is the half-wave voltage, and $(*)$ denotes the complex conjugate. To obtain (7) and (8), it has been assumed that the input RF signals are weak ($|v| \ll v_\pi$). The circuit therefore performs as an I&Q modulator with the lower port E_2 providing the optical carrier modulated by the complex signal and the upper port E_1 providing the optical carrier modulated by the complex conjugate signal. When the modulation is a narrow band RF signal [$v_I = v_{RF}\cos(\omega t + \varphi)$ and $v_Q = v_{RF}\sin(\omega t + \varphi)$], one may write:

$$\begin{bmatrix} E_1 \\ E_2 \end{bmatrix} \approx \frac{1}{2}\left(v_{RF}/v_\pi\right)\pi \begin{bmatrix} i\exp\left[-i\left(\omega t + \varphi\right)\right] \\ -i\exp\left[i\left(\omega t + \varphi\right)\right] \end{bmatrix} A \tag{9}$$

Following the same procedure, if the in-phase RF is applied to the upper MZI modulator and the quadrature RF signal to the lower MZI as before, the output at port D yields:

$$D = -i\left[J_0\left(m\right) + 2J_4\left(m\right)\cos\left(4\omega t\right)\ + 2J_4\left(m\right)\cos\left(-4\omega t\right) + \ldots\right]A \tag{10}$$

where $m = \pi(v_{RF}/v_\pi)$ and the Jacobi-Anger expansion has been used. Equation (10) indicates the n-th order side-bands are suppressed except for n equal to an integer multiple of four. According to the characteristics of the Bessel functions, when the modulation index is $m = 2.40$, the zero-order side-band (i.e., the carrier) is suppressed and the side-bands higher than fourth-order can be ignored without incurring any significant error. When the output of port D is passed through a square-law photo-detector, the circuit performs as a frequency octo-tupler. The versatility of the proposed circuit to perform either as single-side-band modulator or frequency octo-tupler is verified by computer simulations on VPI and illustrated in Figure 2(b).

4. ARCHITECTURE COMPRISING CASCADED MZMS

The proposed circuit architectureshown in Figure 3(a) is formed by an outer Mach-Zehnder interferometer where each of its two arms contains a pair of MZMs in series. The first and second MZI

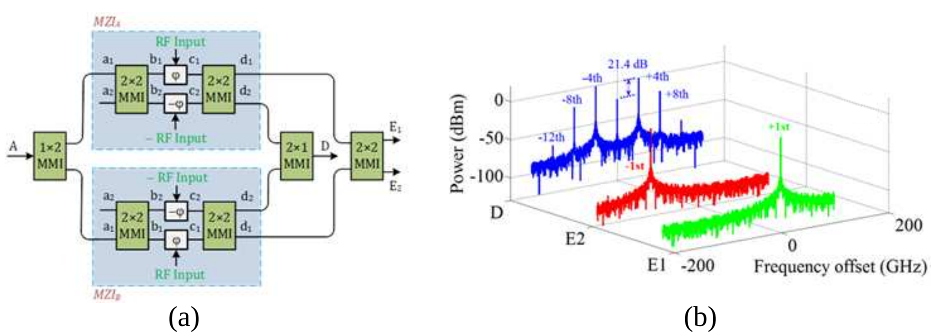

Figure 2: Schematic of a dual-function photonic circuit. (b) Simulated output for frequency octo-tupling and SSB modulation.

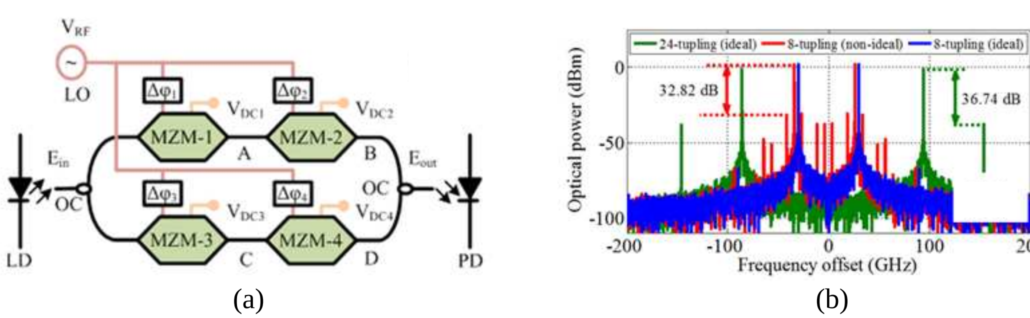

Figure 3: (a) Schematic diagram of the frequency octo-tupler circuit using MZMs in cascade. (b) Simulated output. In (a), labels are: LD: Laser diode; OC: Optical coupler; RF: Radio frequency; LO: RF Local oscillator; PD: Photodiode.

stages are driven in quadrature by the input RF signal. Each arm generates optical sidebands with orders equal to an integer multiple of four. When combined by the outer MZI, the orders equal to an even integer multiple of four are suppressed; only orders equal to an odd integer multiple of four (i.e., ± 4, ± 12, $\pm 20 \ldots$) are unsuppressed. As illustrated in Figure 3(b), after photo-detection the optical output is converted to an electrical current with the strongest oscillatory component at a frequency equal to eight-times the base RF frequency. Note that if the RF drive level is adjusted to suppress the fourth-order optical sidebands, the strongest oscillatory component of the current has a frequency equal to twenty-four times the base RF frequency. Note that the circuit can be operated over a wide range of modulation index ($\sim$2 to $\sim$7.30) as its correct function is not restricted to a particular electrical drive level. In order to maximize the output electrical power of the octo-tupled function, a modulation index of $m = 5.28$ is used in this simulation, which implies a peak RF voltage of $V_{RF} = 1.18V_\pi$, i.e., $\sim$30% less (50% in power) than the voltage required ($V_{RF} = 1.68V_\pi$) for same modulation index in [4, 5] that uses the single-stage parallel MZM configuration.

5. CONCLUSION

Various photonic circuit architectures for RF frequency multiplication and frequency translation have been presented. Firstly a systematic design method for the suppression of unwanted harmonics produced by arrays of N-parallel phase modulators electrically driven with a progressive $2\pi/N$ phase shift has been presented. Secondly, a photonic circuit architecture capable of implementing frequency up-conversion and frequency octo-tupling has been proposed and verified by computer simulations. The circuit requires no DC-bias as the static phase shifts are introduced by using the intrinsic relative phase relations between the output and input ports of MMI couplers. Last but never the least, a photonic circuit architecture featuring two-stage MZM architecture has been proposed for frequency octo-tupling and 24-tupling. The analysis and simulations prove this cascade architecture is advantageous compared to the single-stage parallel MZM configuration with equivalent function because it requires 3-dB less power in RF drive.

REFERENCES

1. Qi, G., J. Yao, J. Seregelyi, S. Paquet, and C. Bélisle, "Generation and distribution of a wide-band continuously tunable millimeter-wave signal with an optical external modulation technique," *Transactions on Microwave Theory and Techniques*, Vol. 53, No. 10, 3090–3097, 2005.
2. Li, W. and J. Yao, "Microwave generation based on optical domain microwave frequency octupling," *Photonics Technology Letters*, Vol. 22, No. 1, 24–26, 2010.
3. Zhu, Z., S. Zhao, Y. Li, X. Chu, X. Wang, and G. Zhao, "A radio-over-fibre system with frequency 12-tupling optical millimeter-wave generation to overcome chromatic dispersion," *Quantum Electronics Letters*, Vol. 49, No. 11, 919–922, 2013.
4. Hasan, M., R. Guemri, R. Maldonado-Basilio, F. Lucarz, J.-L. de Bougrenet, and T. J. Hall, "Photonic integrated circuit for frequency 8- and 24-tupled millimeter wave signal generation," *Optics Letters*, Vol. 39, No. 24, 6950–6953, 2014.
5. Hasan, M., R. Maldonado-Basilio, and T. J. Hall, "Short communication," *Journal of Modern Optics*, in Print, 2015.
6. Maldonado-Basilio, R., M. Hasan, H. Nikkhah, S. Abdul-Majid, R. Guemri, F. Lucarz, J.-L. Bougrenet de la Tocnaye, and T. J. Hall, "Electro-optic up-conversion mixer amenable to photonic integration," *Journal of Modern Optics*, Accepted, 2015.